

AD-A207 557

TECHNICAL REPORT TR-RD-SS-88-10

APPLICATION OF CRYSTAL LATTICE DISINTEGRATION CRITERIA
TO COMPUTE MINIMUM SHOCK INDUCED REACTIVE CONDITIONS
IN SOLID EXPLOSIVES AND INERT MATERIALS

James P. Billingsley
Carl L. Adams
Systems Simulation and Development Directorate
Research, Development, and Engineering Center

March 1989



U.S. ARMY MISSILE COMMAND

Redstone Arsenal, Alabama 35898-5000

Approved for public release; distribution is unlimited.

DTIC
ELECTE
APR 21 1989
S H D

0 89 4 21 025

DISPOSITION INSTRUCTIONS

**DESTROY THIS REPORT WHEN IT IS NO LONGER NEEDED. DO NOT
RETURN IT TO THE ORIGINATOR.**

DISCLAIMER

**THE FINDINGS IN THIS REPORT ARE NOT TO BE CONSTRUED AS AN
OFFICIAL DEPARTMENT OF THE ARMY POSITION UNLESS SO DESIGNATED
BY OTHER AUTHORIZED DOCUMENTS.**

TRADE NAMES

**USE OF TRADE NAMES OR MANUFACTURERS IN THIS REPORT DOES
NOT CONSTITUTE AN OFFICIAL INDORSEMENT OR APPROVAL OF
THE USE OF SUCH COMMERCIAL HARDWARE OR SOFTWARE.**

REPORT DOCUMENTATION PAGE				Form Approved OMB No 0704-0188 Exp Date Jun 30, 1986	
1a. REPORT SECURITY CLASSIFICATION Unclassified			1b. RESTRICTIVE MARKINGS		
2a. SECURITY CLASSIFICATION AUTHORITY			3. DISTRIBUTION/AVAILABILITY OF REPORT Approved for public release; distribution is unlimited.		
2b. DECLASSIFICATION/DOWNGRADING SCHEDULE					
4. PERFORMING ORGANIZATION REPORT NUMBER(S) TR-RD-SS-88-10			5. MONITORING ORGANIZATION REPORT NUMBER(S)		
6a. NAME OF PERFORMING ORGANIZATION Sys Sim and Dev Dir, Res, Dev, and Engr Ctr		6b. OFFICE SYMBOL (if applicable) AMSMI-RD-SS	7a. NAME OF MONITORING ORGANIZATION		
6c. ADDRESS (City, State, and ZIP Code) Commander U.S. Army Missile Command ATTN: AMSMI-RD-SS Redstone Arsenal, AL 35898-5252			7b. ADDRESS (City, State, and ZIP Code)		
8a. NAME OF FUNDING/SPONSORING ORGANIZATION		8b. OFFICE SYMBOL (if applicable)	9. PROCUREMENT INSTRUMENT IDENTIFICATION NUMBER		
8c. ADDRESS (City, State, and ZIP Code)			10. SOURCE OF FUNDING NUMBERS		
			PROGRAM ELEMENT NO.	PROJECT NO.	TASK NO.
11. TITLE (Include Security Classification) APPLICATION OF CRYSTAL LATTICE DISINTEGRATION CRITERIA TO COMPUTE MINIMUM SHOCK INDUCED REACTIVE CONDITIONS IN SOLID EXPLOSIVES AND INERT MATERIALS					
12. PERSONAL AUTHOR(S) James P. Billingsley and Carl L. Adams					
13a. TYPE OF REPORT Final		13b. TIME COVERED FROM Aug 87 TO Aug 88	14. DATE OF REPORT (Year, Month, Day) March 1989		15. PAGE COUNT 34
16. SUPPLEMENTARY NOTATION					
17. COSATI CODES			18. SUBJECT TERMS (Continue on reverse if necessary and identify by block number)		
FIELD	GROUP	SUB-GROUP	Explosive Comp-B H-6 Lattice Fracture		
			Detonation TNT Plexiglass Shocked Solids		
			Comp-B3 PBX-9404 Crystal Lattice		
19. ABSTRACT (Continue on reverse if necessary and identify by block number) A threshold particle velocity criteria derived by E. R. Fitzgerald [2] for the beginning of crystal lattice breakup and disintegration has been applied to shocked explosives and an inert material. In shocked explosives, reactions leading to detonation occur above a certain "threshold" magnitude. The computed crystal lattice breakup shock pressures compare rather well with observed experimental "threshold" shock pressures for six high explosives. The six explosives are: Comp-B3, Comp-B, TNT, PBX-9404, Teteryl, and H-6. In addition, the crystal lattice breakup criteria provides an explanation for the observed lowering of the detonation "threshold" shock pressure as the explosives are made more porous or less dense. Finally, the shock pressures, at which output from thermocouples embedded in shocked materials (PEX-9404 and Plexiglass) increases dramatically, compare favorable with predictions based on crystal lattice disintegration criteria. (Continued)					
20. DISTRIBUTION/AVAILABILITY OF ABSTRACT <input type="checkbox"/> UNCLASSIFIED/UNLIMITED <input checked="" type="checkbox"/> SAME AS RPT. <input type="checkbox"/> DTIC USERS			21. ABSTRACT SECURITY CLASSIFICATION Unclassified		
22a. NAME OF RESPONSIBLE INDIVIDUAL Dr. James P. Billingsley			22b. TELEPHONE (Include Area Code) (205) 876-5210		22c. OFFICE SYMBOL AMSMI-RD-SS-AA

BLOCK 19 (Continued):

Consequently, it is tentatively concluded that crystal lattice breakup, or self-sustained phonon fission as Fitzgerald calls it, is responsible for the initiation of detonation in shocked explosives and enhanced thermocouple output in shocked materials.

Several recommendations for future work are given.

TABLE OF CONTENTS

Section	Page
I. INTRODUCTION.....	1
II. FITZGERALD'S CRYSTAL LATTICE FRACTURE OR DISINTEGRATION PARTICLE VELOCITY CRITERIA.....	2
III. MINIMUM CRYSTAL LATTICE FRACTURE SHOCK VELOCITY AND SHOCK PRESSURE.....	3
IV. THEORETICAL AND EXPERIMENTAL REACTION THRESHOLD SHOCK CONDITIONS FOR EXPLOSIVES AND INERT MATERIALS.....	5
V. CONCLUSIONS.....	6
IV. RECOMMENDATIONS.....	7
REFERENCES.....	17
APPENDIX. COMPUTATION OF m_{av} AND d_{lav} FOR CHEMICAL COMPOUNDS AND MIXTURES OF COMPOUNDS.....	A-1



Accession For	
NTIS GRA&I	<input checked="" type="checkbox"/>
DTIC TAB	<input type="checkbox"/>
Unannounced	<input type="checkbox"/>
Justification	
By	
Distribution/	
Availability Codes	
Dist	Avail and/or Special
A-1	

I. INTRODUCTION

While engaged in a study of solid explosive detonation via small projectile impact, Reference [1], a scheme was developed to theoretically compute the lowest one-dimensional shock pressure required to initiate reactions leading to detonation in a solid explosive.

A threshold particle velocity criteria derived by E. R. Fitzgerald [2] for the onset of crystal lattice disintegration has been shown to agree rather well with the lowest particle velocity, and hence, shock velocity and/or shock pressure required to initiate reactions leading to detonation in certain explosives. In addition, the relation has also been employed to compute the lattice breakup shock conditions for an inert nonexplosive material, polymethyl methacrylate (PMMA). This result agreed well with an experimentally observed shock pressure level; above which shocked thermocouple output increased rapidly with increased shock pressure.

Similar shocked thermocouple data were also available for one explosive, PBX-9404. The computed lattice breakup shock pressure for PBX-9404 agrees rather well with both the pressure level for increased thermocouple response, and the experimental shock pressure necessary to initiate reactions leading to detonation.

It is known that a porous explosive requires less shock pressure to initiate detonation than the same explosive which is less porous or more dense. It is shown analytically and numerically that the shock pressures (or particle velocity) necessary for crystal lattice breakup also decreases as the material density decreases. This is suggested as an explanation of the observed porosity sensitivity effect.

Although additional investigation is needed, it is tentatively concluded that the onset of crystal lattice disintegration is responsible for reactions leading to detonation of explosions via shock pressure input. Also, it is physically plausible that crystal lattice fracture is responsible for the enhanced thermocouple response above a certain pressure level in shocked materials.

II. FITZGERALD'S CRYSTAL LATTICE FRACTURE OR DISINTEGRATION PARTICLE VELOCITY CRITERIA

From particle dynamics considerations, Fitzgerald ([2], Chapter III) derived the following relation for the velocity of a particle (in a crystal lattice) necessary to produce lattice disintegration. He called this the phonon fission velocity, V_f , which is:

$$V_f = \frac{V_l + \sqrt{V_l^2 + 4 * V_l * C_s}}{2} \quad (1)$$

It is approximately equal to:

$$V_f = \sqrt{V_l * C_s} \quad (2)$$

the velocities V_l and C_s are defined as follows:

$$V_l = \frac{h}{2 m d_l} \quad (3)$$

= limiting free particle velocity which can occur without permanent lattice deformation (plastic flow); or the limit propagation velocity for particle-momentum waves in a stationary lattice.

$$C_s = \sqrt{\frac{2 * C_t^2 + C_l^2}{6}} \quad (4)$$

= A mean sound velocity defined such that the dissociation energy of an atom of mass, m , is $m C_s^2$

The quantities appearing on the right-hand side of Equations (Eqs.) (3) and (4) are defined as follows:

h = Planck's constant

$$= 6.626196 \times 10^{-27} \frac{(\text{gram}) (\text{cm}^2)}{\text{sec}}$$

d_l = Closest distance between the atoms in a crystal lattice, or the atomic spacing in a slip direction. Units are angstrom units, \AA ($\text{\AA} = 10^{-8} \text{ cm}$)

m = Mass of one atom, grams.

C_t = Elastic transverse or shear wave velocity, $\text{cm}/\mu - \text{sec}$

C_l = Elastic longitudinal wave velocity, $\text{cm}/\mu - \text{sec}$

With respect to V_f , Fitzgerald points out that self-sustained fission is possible if fragments of the broken lattice strike other lattice sections and the process is repeated. Then he says: "The explosive nature of certain fractures may arise from this source," ([2], p. 81).

III. MINIMUM CRYSTAL LATTICE FRACTURE SHOCK VELOCITY AND SHOCK PRESSURE

Consequently, it seemed likely that lattice breakup phenomena could also initiate reactions leading to detonation in explosives. If so, then V_f would be the minimum particle velocity (due to impact or shock) required to cause detonation for one-dimensional large sample conditions. The corresponding shock velocity, U_{sf} , and shock pressure, P_{sf} , are:

$$U_{sf} = C_0 + S * V_f \quad (5)$$

$$P_{sf} = \rho_0 U_{sf} V_f \quad (6)$$

With respect to Eq. 5, experimental results reveal that the shock velocity is a linear function of the particle velocity for many materials. C_0 and S (a constant) have been determined for many metals, plastics, and explosives ([3] through [7]). C_0 is a constant also, and is equal to the bulk sound velocity for most materials. The shock velocity may be a nonlinear function of the particle velocity for certain substances. In that case, U_g can be found from tables or graphs of U_g as a function of U_p . Table 1 contains C_0 and S information for the shocked explosives and materials considered in this report. The sources of this information are also listed.

Equation (6) is the well known expression for shock pressure. P_{sf} is the product of the material density (ρ_0), shock velocity (U_{sf}), and the particle velocity (V_f).

Numerical values of the three quantities, V_f , U_{sf} , and P_{sf} may, thus, be computed and compared with experimental data for any phenomena which might be associated with lattice disintegration.

The particle fracture velocity V_f , is a function of two velocities, V_1 , and C_s , via Eqs. (1) or (2). The computation of V_1 requires the knowledge of two quantities, m , and d_1 . For the compounds and mixtures considered herein, m is m_{av} , the average weight of a single atom in the material. It is a constant for a given material and can be computed from the chemical formula or composition information. The distance d_1 will be a function of the density or specific weight (ρ_0) and m_{av} . It is computed as follows:

$$N_v = \frac{\rho_0}{m_{av}} = \frac{\frac{(\text{Grams})}{\text{cm}^3}}{\frac{(\text{Grams})}{\text{Atom}}} = \frac{\text{Atoms}}{\text{cm}^3} \quad (7)$$

Considering that each atom, on the average, occupies a small cube whose side is d_1 , then

$$d_1^3 = \frac{1}{N_V} = \frac{m_{av}}{\rho_0} = \text{cm}^3 \quad (8)$$

$$d_1 = \left(\frac{m_{av}}{\rho_0} \right)^{1/3} = \text{cm} \quad (9)$$

Thus, from Eqs. (3) and (9):

$$V_1 = \frac{h (\rho_0)^{1/3}}{2 (m_{av})^{4/3}} \quad (10)$$

Since h is a constant, and for a given material, m_{av} is a constant, then:

$$V_1 = K (\rho_0)^{1/3} \quad (11)$$

Where:

$$K = \frac{h}{2 (m_{av})^{4/3}} \quad (12)$$

From Eq. (11), V_1 will decrease as the density decreases, or as the material becomes more porous.

The elastic wave velocities, C_1 and C_t , will normally decrease as the density decreases also. Thus, from Eq.(4), C_s will also decrease as the material becomes less dense or more porous.

It follows, then, from Eqs. (1) and (2), that V_f will decrease as the density decreases or porosity increases.

The shock velocity, U_{sf} , will be affected by porosity also; not only by the V_f or particle velocity contribution (Eq. (5)), but the form of the relationship may change. In general, the shock velocity will decrease (for a given particle velocity) as the density decreases or porosity increases. Note the characteristics of Tetrayl described in [20].

Finally, the lattice fracture shock pressure, P_{sf} , will decrease via the product $(\rho_0 * U_{sf} * V_f)$ as the density decreases and porosity increases.

The variation of V_f , U_{sf} , and P_{sf} with material density (ρ_0) has an important implication which will be discussed in Section IV.

Refinements, with respect to the computation of V_1 , appear feasible. Particular atoms or combinations of atoms and their associated minimum slip distances, d_1 , could be given special attention.

IV. THEORETICAL AND EXPERIMENTAL REACTION THRESHOLD SHOCK CONDITIONS FOR EXPLOSIVE AND INERT MATERIALS

V_f , U_{gf} , and P_{gf} were computed for six high explosives and one inert material for comparison with selected experimental results. The six explosives were: Comp-B3, Comp-B, TNT (pressed), PBX-9404, Tetryl, and H-6. The inert material was Plexiglas II, UVA, which is also called PMMA. The pertinent results from the computations are listed in Table 2. Reference [7] supplied vital information (chemical composition, longitudinal and transverse elastic wave velocities) for the explosives. Reference [6] supplied this information for the PMMA. Appendix A contains the computations for m_{av} and d_{lav} for the explosives and PMMA.

Table 3 lists the computed U_{gf} and P_{gf} results along with pertinent experimental information. Much of the experimental information came from explosive shock pressure sensitivity tests such as the:

1. Large scale Gap Tests, LSGT [9]
2. Low Amplitude Shock Initiation Tests, LAST [10]
3. Modified Gap Test, [8], [13]
4. Small Scale Gap Tests, SSGT, [19]

Some very important experimental data came from [11] and [12]. Reference [11] documents a detailed investigation of burning and buildup to detonation in pressed TNT. Shock pressures were generated by impacting the explosives with aluminum plates. The results were also employed in [12] for an analysis of the critical energy concept. In addition, [12] also contains shock velocity information acquired via an explosive wedge technique. This yielded a significant data point which compared well with U_{gf} for TNT.

References [14] and [15] document thermocouple temperature measurements in shocked materials. PBX-9404 [14], and PMMA [15], were instrumented with thermocouples and shock loaded at various levels via impact. Above a threshold pressure, the thermocouple maximum output increases rapidly with small increases in shock pressure for both of these materials. These threshold pressure points are listed in Table 3 along with the computed value for P_{gf} . The magnitude comparison is quite good for the PBX-9404, and almost one-to-one for the PMMA.

To facilitate an overall quick visual comparison, Figure 1 illustrates both the computed P_{gf} and the experimental large reaction shock pressure data referred to above and listed in Table 3. In general, P_{gf} is either bracketed by the experimental results or compares rather well with a single experimental point.

It is well known that porosity affects the sensitivity of an explosive to shock induced detonation. In general, less shock pressure is required as the explosive density is decreased or the porosity increases. For examples, see [9], (Figure 4), and [11], [12], and [19]. This observed detonation sensitivity phenomena is believed to be caused by the decrease in V_f , U_{gf} , and P_{gf} as the density decreases. (Section III).

To compute V_f , and hence U_{sf} and P_{sf} , V_l and C_s must be known as a function of ρ_0 . V_l is easy to compute via Eq. (10). C_s is a function of C_l and C_t and these wave velocities will vary with ρ_0 . Sources for C_l and C_t as a function of density for the materials considered herein were unknown to the authors.

Thus, strictly speaking, precise or consistent values of C_s , V_f , U_{sf} , and P_{sf} as a function of material density could not be computed. However, for Tetryl, a consistent computation was made for one density ($\rho_0 = 1.68$ Grams/cc) and an approximate computation was made for another density ($\rho_0 = 1.50$ Grams/cc) (Table 2). V_l was computed correctly, but C_s was the same for both densities since C_l and C_t for $\rho_0 = 1.68$ Grams/cc was utilized in each case. This makes V_f , U_{sf} , and P_{sf} slightly high for the more porous Tetryl ($\rho_0 = 1.50$ Gram/cc). P_{sf} for both of these densities is plotted in Figure 2 where they are compared with both LSGT [9] and SSGT [19] results. The comparison is quite good, even though P_{sf} for $\rho_0 = 1.5$ Grams/cc is somewhat less than shown.

Figure 3 compares the single P_{sf} point computed for TNT ($\rho_0 = 1.635$ Grams/cc) with available reactive pressure test results acquired for various densities. P_{sf} is less than the comparable equal density SSGT and LSGT results. However, P_{sf} agrees rather well with the reactive (P_R) and detonation threshold (P_D) pressure results reported in [11] which was acquired via aluminum projectile impact testing.

V. CONCLUSIONS

Although this is certainly not an exhaustive investigation, enough information has been presented to indicate that the threshold shock pressures required to initiate reactions leading to detonations in explosives may be related to a critical particle velocity, V_f , sufficient to cause crystal lattice fracture, breakup, and disintegration. Theoretical and experimental results have compared rather well for six high explosives.

The trend of the experimentally observed minimum shock pressure to initiate detonation in explosives as a function of density is consistent with the variation of the crystal lattice fracture shock pressure, P_{sf} , with material density. It is shown analytically that P_{sf} decreases as density (ρ_0) decreases, and it is known via experiments that the shock magnitude to cause detonation decreases as the explosive becomes more porous [9] and [19]. P_{sf} computations compare reasonably well with experimental results.

In addition, it has been shown for two materials (PBX-9404 and PMMA) that the shock level at which a greatly enhanced thermocouple output was observed coincides rather well with the computed lattice fracture shock pressure, P_{sf} . In fact for PBX-9404, P_{sf} , P_D (detonation threshold), and P_R (thermocouple reaction threshold), are all relatively close together. Thus, it is strongly suspected that lattice disintegration and self-sustained phonon fission cause the noticeable increase in temperature and this creates chemical reactions which quickly escalate to detonation. Consequently, it is suggested that other explosives, particularly pressed TNT and Tetryl, be instrumented with thermocouples and tested in the same manner as delineated in [14] and [15].

It is very plausible from a physical viewpoint that crystal lattice disintegration would cause an observable reaction in shocked solids. The rather limited results of this investigation indicate that this phenomena may be responsible for shock induced detonation of solid explosives, and the rather large thermoelectric response of shocked solid materials. Certain observed phase changes in shock loaded materials may be caused by crystal lattice disintegration.

VI. RECOMMENDATIONS

Some recommendations for additional work have already been made, either explicitly, or implicitly in the previous sections. For easy reference, these are restated here and some additional recommendations are made.

A. In addition to PMMA (Plexiglas II, UVA), [15] also contained thermocouple response information for a shocked epoxy, EPON 828. A threshold pressure for enhanced thermocouple output was observed for this material. For comparison, V_f , U_{sf} , and P_{sf} should be computed for EPON 828. This will be done as soon as possible.

B. In a manner similar to that described in [14] and [15], Comp-B3, Comp-B, pressed TNT, Tetryl, and H-6 should be instrumented with thermocouples and shock loaded at various levels. If the present postulations are valid, these explosives would exhibit an increase in thermocouple response near the P_{sf} pressure level.

C. Tests have been conducted on pure metals (iron, copper, and aluminum) which were instrumented with thermocouples and shock loaded to rather high pressures via impact [16] and [17]. Similar tests should be systematically conducted at lower shock pressures (30 to 150 kilobars) to ascertain if they exhibit a thermocouple output pressure threshold response point such as observed for PMMA and PBX-9404 near the computed P_{sf} magnitude. V_f values for iron, copper and aluminum are given in [2]. Shock and particle velocity information (C_0 and S) for these metals are given in [3]. Thus, P_{sf} , for iron, copper and aluminum can be computed and compared with any appropriate experimental results. This would provide a severe test for the crystal lattice fracture shock pressure, P_{sf} , criteria.

D. Information on the variation of the longitudinal (C_l) and transverse (C_t) elastic wave velocities as a function of density for certain explosives should be acquired, via experimentation if necessary. Information on the variation of U_s , V_s , and U_p as a function of density is also required. Then exact values of V_s , U_{sf} , and P_{sf} as a function of density could be computed and compared with experimental data such as shown in Figures 2 and 3.

E. The computation of V_l via Eq. (3), could possibly be refined to take into account atoms and combinations of atoms, and their associated minimum crystal lattice slip distance, which might warrant special attention. This, of course, applies to compounds and mixtures. In the present investigation, average values were computed for the mass of an atom and the distance between them. See Appendix A for these calculations. More sophisticated computations of m_{av} and d_l , should be attempted, for example, to delineate differences in heterogeneous and homogeneous materials.

F. Permanent lattice distortion or plastic flow occurs for particle velocities between V_l (Eq. (3)) and V_f (Eq. (1)). Consequently, reactions in explosives (ignition, burning, and even detonation) can occur in this regime. This is a prime topic for further investigation.

G. The present analysis has not addressed any transient or time dependent phenomena such as the critical energy criteria [18]. However, an investigation, based on concepts presented in [2], should be done to ascertain if the observed time dependence is related to the particle wave motion in a lattice structure.

H. Reference [21], with its comprehensive review and reference list, is a prime source of topics which should be investigated with respect to shocked crystal lattice disintegration influences. For instance, the authors believe that certain solid-stated shock induced phase changes [22], and shock induced increased chemical reactivity [23], may be caused by the crystal lattice fragmentation phenomena. Lattice breakup and its accompanying self-sustained phonon fission and increased heating are plausible physical conditions for phase changes, increased chemical reactivity, and different electronic characteristics to occur.

TABLE 1. Shocked Material Information.

<u>MATERIAL</u>	<u>ρ_0</u> <u>Grams</u> <u>cm³</u>	<u>C_0</u> <u>cm</u> <u>μ-sec</u>	<u>S</u> -	<u>SOURCE</u> -
Comp-B3	1.700	0.303	1.73	Ref. [4]
Comp-B	1.700	0.295	1.67*	Ref. [4]
TNT (Pressed)	1.635	0.208	2.35	Ref. [5]
PBX-9404	1.842	0.245	2.48	Ref. [5]
H-6	1.750	0.283	1.70	Ref. [7]
Plexiglas II, UVA (PMMA)	1.180	0.268	1.61	Ref. [6]
Tetryl	1.70	0.2476	1.416	Ref. [20]
Tetryl**	1.50	0.020	4.50	Ref. [20]

*S was modified from 1.58 to 1.67.

** For this density, U_g versus U_p for Tetryl is nonlinear, however, for shock velocities less than 0.19 cm/ μ -sec the above linearization matches the experimental data.

TABLE 2. Numerical Results for V_f , U_{sf} and P_{sf} .

Material	m_{av} App.-A GRAMS $\times 10^{-23}$	d_l App.-A CM 10^{-8}	V_l Eq. 3 $\frac{CM}{\mu\text{-sec}}$	C_l $\frac{CM}{\mu\text{-sec}}$	C_t $\frac{CM}{\mu\text{-sec}}$	C_s Eq. 4 $\frac{CM}{\mu\text{-sec}}$	V_f Eq. 1 $\frac{CM}{\mu\text{-sec}}$	U_{sf} Eq. 5 $\frac{CM}{\mu\text{-sec}}$	P_{sf} Eq. 6 KBARS
COMP-83	1.7700	2.1839	0.008571 $\rho_0=1.70$	0.3120	0.1710	0.1612 $\rho_0=1.726$	0.04170	0.3751	26.59
COMP-B	1.7494	2.1751	0.008228 $\rho_0=1.70$	0.3120	0.1710	0.1612 $\rho_0=1.726$	0.04077	0.3631	25.16
TNT (PRESSED)	1.7960	2.2229	0.008299 $\rho_0=1.635$	0.2580	0.1350	0.1310 $\rho_0=1.635$	0.03739	0.2959	18.09
PBX-9404	1.7571	2.1235	0.008879 $\rho_0=1.835$	0.2900	0.1570	0.1491 $\rho_0=1.84$	0.04109	0.3469	26.16
H-6	1.8849	2.2085	0.007959 $\rho_0=1.75$	0.2460	0.1550	0.1345 $\rho_0=1.75$	0.03903	0.3494	34.87
PLEXIGLAS I, OVA	1.9933	2.1099	0.01417 $\rho_0=1.18$	0.2711	0.1373	0.1161 $\rho_0=1.18$	0.05157	0.3510	21.36
TETRYL $\rho_0=1.68$	1.9072	2.2475	0.007729 $\rho_0=1.68$	0.2270	0.1240	0.1165 $\rho_0=1.68$	0.03411	0.2959 $\rho_0=1.68$	17.00
TETRYL* $\rho_0=1.50$	1.9072	2.3340	0.007443 $\rho_0=1.50$	0.2270	0.1240	0.1165 $\rho_0=1.68$	0.03543	0.1794 $\rho_0=1.50$	9.53

* V_f , U_{sf} , and P_{sf} for this porous Tetryl are slightly high since longitudinal (C_l) and Transverse (C_t) wave velocity data for Tetryl with $\rho_0 = 1.68$ Gram/cm³ were employed to compute C_s and V_f .

TABLE 3. Theoretical and Experimental Reactive Shock Information Tabulation.

Material	U_{sf} TABLE 2 $\frac{\text{cm}}{\mu\text{-sec}}$	P_{sf} TABLE 2 KBar	Exper. Data cm/ μ -sec or KBar	Exper. Source -	Remarks WRT Exper. Data - -
Comp-B3 $\rho_0 = 1.71$ G/cc	0.3751	26.59	$P_D = 22.0$	Ref. 9 (TABLE 11)	Critical detonation initiating pressure from LSGT* $\rho_0 =$ 1.72 G/cc
			$P_R = 33.0$	Ref. 10 (Fig. 7)	Large reaction threshold in LASI tests** $\rho_0 = 1.702$ G/cc
Comp-B $\rho_0 = 1.71$ G/cc	0.3631	25.16	$P_D = 24.1$	Ref. 9 (TABLE 11)	Critical detonation initiating pressure from LSGT. $\rho_0 =$ 1.70 G/cc
TNT (Pressed) $\rho_0 = 1.635$ G/cc	0.2959	18.09	$P_R = 14.0$	Ref. 11 (Fig. 4)	Coarse Grain $\rho_0 = 1.55$ G/cc
			$P_R = 15.0$ $P_D = 16.1$	Ref. 11 (Fig. 4)	Fine Grain $\rho_0 = 1.55$ G/cc
			$U_s = 0.31$	Ref. 12 (Fig. 10)	Assymtotic shock velocity for both coarse and fine grains. $\rho_0 =$ 1.55 G/cc
			$P_g = 24.0$	Ref. 9 (App. C)	P_g from LSGT. $\rho_0 = 1.60$ G/cc (97% TMD)
			$P_g = 26.0$	Ref. 9 (App. C)	P_g from LSGT $\rho_0 = 1.640$ G/cc (99% TMD)
			$P_{GR} = 20.0$	Ref. 13*** (Fig. 5) (TABLE 2)	Reaction, Mod. Gap Test, $\rho_0 = 1.60$ G/cc
			$P_{CD} = 25.0$ to 30.0	Ref. 13 (Fig. 5) (TABLE 2)	Detonation, Mod. Gap Tests, $\rho_0 = 1.60$ G/cc
PBX-9404 $\rho_0 = 1.835$ G/cc	0.3469	26.16	$P_R = 30.0$	Ref. 14	Large Reaction thresh- old for thermocouple response $\rho_0 = 1.84$ G/cc
			$P_B = 16.0$ $P_D = 34.0$	Ref. 8 (TABLE 2) Ref. 8 (TABLE 2)	Burning, $\rho_0 =$ 1.83 G/cc Detonation, $\rho_0 = 1.83$ G/cc

TABLE 3. Theoretical and Experimental Reactive Shock Information
Tabulation. (Continued)

Material	U_{sf} cm μ-sec	P_{sf} KBar	Exper. Data cm/μ-sec or KBar	Exper. Source	Remarks WRT Exper. Data
H-6 $\rho_0 = 1.75$ G/cc	0.3494 (TABLE 2)	23.87 (TABLE 2)	$P_g = 21.0$	Ref. 10 (Fig. 9)	P_g from LSGT $\rho_0 = 1.77$ G/cc
			$P_R = 40.0$	Ref. 10 (Fig. 9)	Large reaction threshold in LASI tests $\rho_0 = 1.77$ G/cc
			$P_g = 20.0$	Ref. 9 (App. C)	P_g from LSGT $\rho_0 = 1.76$ G/cc PRESSED H-6
			$P_g = 30.0$	Ref. 9 (App. C)	P_g from LSGT $\rho_0 = 1.75$ G/cc Cast H-6
Plexiglas II, UVA (PMMA) $\rho_0 = 1.18$ G/cc	0.3510 (TABLE 2)	21.36 (TABLE 2)	$P_R = 20.0$	Ref. 15 (Fig. 5)	Large Reaction Threshold for thermocouple output. $\rho_0 = 1.18$ G/cc
Tetryl $\rho_0 = 1.68$ G/cc	0.2959 (TABLE 2)	17.00 (TABLE 2)	$P_g = 15.5$	Ref. 9 (Fig. 4)	LSGT, Estimated $\rho_0 = 1.68$ G/cc
			$P_{50} = 17.5$	Ref. 19 (P. C1A1)	SSGT,**** Exp. Data $\rho_0 = 1.687$ G/cc
Tetryl $\rho_0 = 1.50$ G/cc	0.1794 (TABLE 2)	9.53 (TABLE 2)	$P_g = 10.0$	Ref. 9 (Fig. 4 and App. C)	P_g from LSGT $\rho_0 = 1.491$ G/cc

* LSGT - Large Scale Gap Tests (Ref. 9).

** LASI - Low Amplitude Shock Initiation Tests (Ref. 10).

*** Reference 13 states that P_{GR} (Reaction Pressure) is sufficient
to cause detonation, if the specimen is large enough.

**** SSGT - Small Scale Gap Tests (Ref. 19).

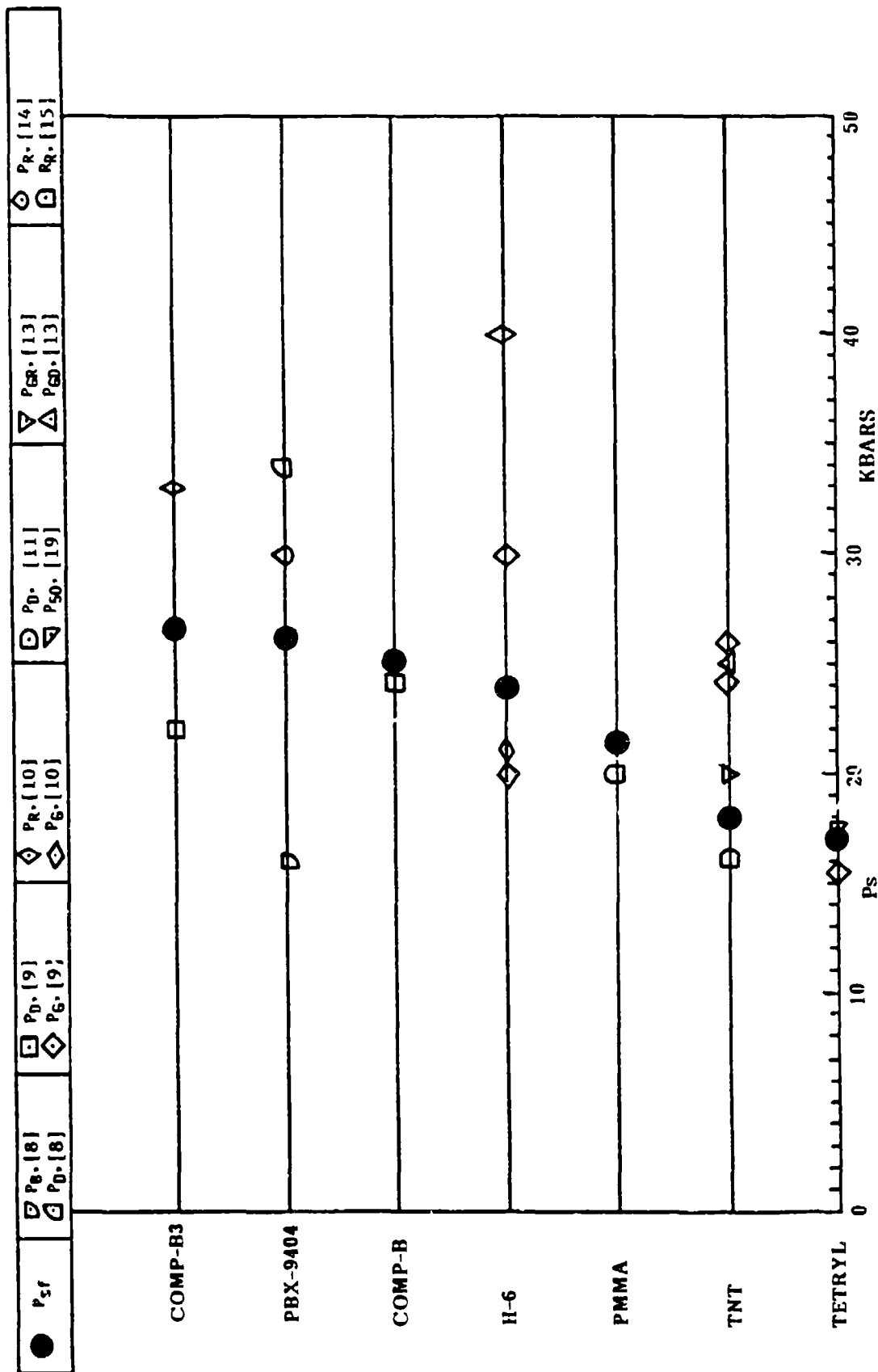


Figure 1. Theoretical and experimental reactive shock pressures.

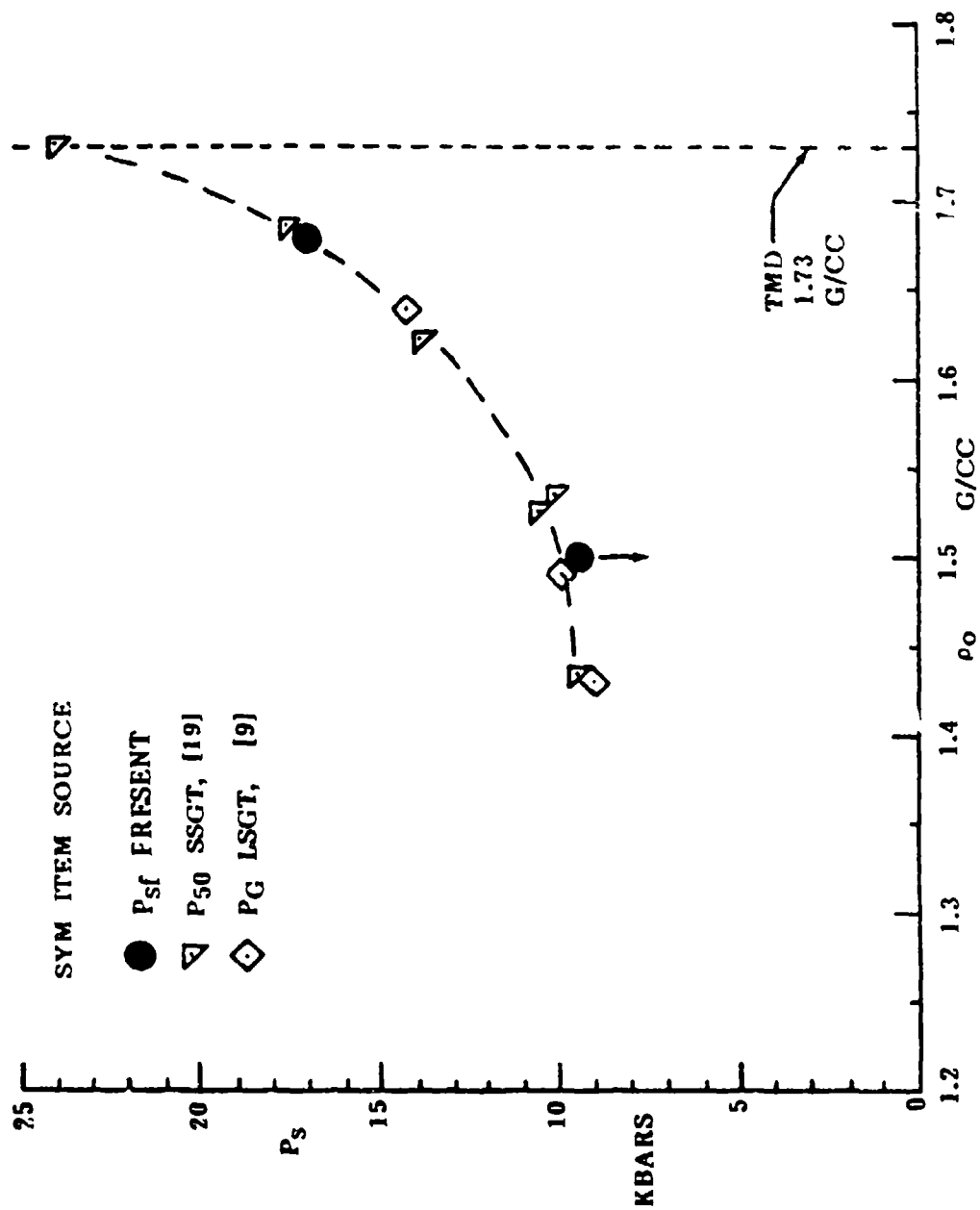


Figure 2. P_{SF} comparison with test results for tetryl.

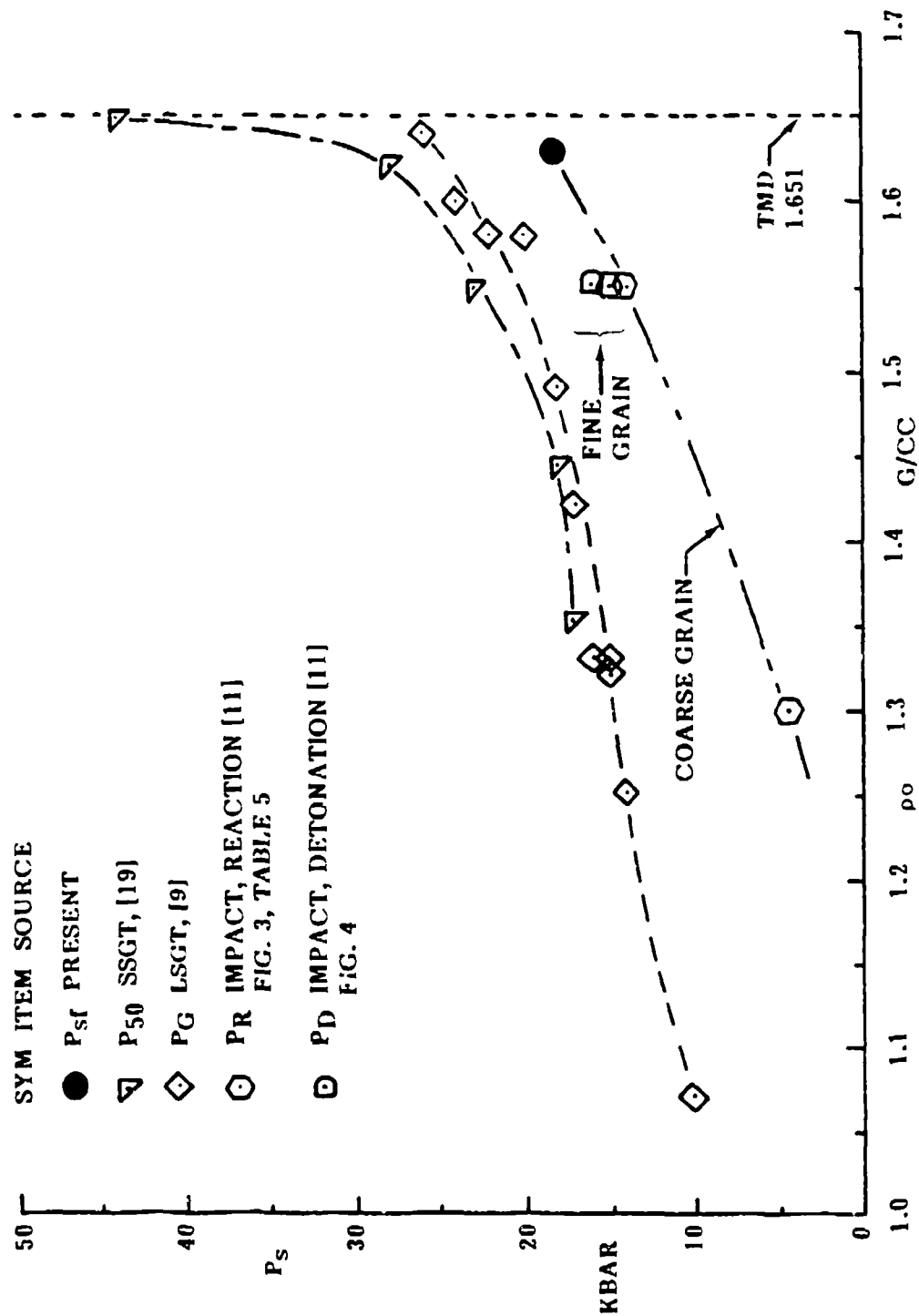


Figure 3. P_{sf} comparison with test results for pressed TNT.

REFERENCES

1. Billingsley, J. P., and Adams, C. L., "Remarks on Certain Aspects of Solid Explosive Detonation via Small Projectile Impact," Special Report RD-SS-88-11, (to be published), Aeroballistics Analysis Branch, Systems Simulation and Development Directorate, Research Development and Engineering Center, U.S. Army Missile Command, Redstone Arsenal, AL, 35898.
2. Fitzgerald, E. R., Particle Waves and Deformation of Crystalline Solids, Interscience Publishers, a Division of John Wiley and Sons, Inc., New York, 1966.
3. McQueen, R. G., Marsh, S. P., Taylor, J. W., Fritz, J. N., and Carter, W. M., "The Equation of State of Solids from Shock Wave Studies," Hypervelocity Impact Phenomena, Edited by Ray Kinslow, Academic Press, New York, 1970, pp. 293-417, and also Appendices A, B, C, D, and E of this book, pp. 515-568.
4. Jameson, R. L., Boyle, V. M., and Sultanoff, M., "Determination of Shock Hugoniot for Several Condensed Phase Explosives," paper presented at the Fourth Symposium (International) on Detonation, 12-15 October 1965, proceedings published as ACR-126, pp. 241-247, by the Office of Naval Research, Department of the Navy, Washington, DC.
5. Ramsey, J. B., and Popolato, A., "Analysis of Shock Wave and Initiation Data for Solid Explosives," paper presented at the Fourth Symposium (International) on Detonation, 12-15 October 1965, published as ACR-126, pp. 233-238, Office of Naval Research, Department of the Navy, Washington, DC.
6. Deal, W. E., "Shock Wave Research On Inert Solids," an invited review in The Fourth Symposium (International) on Detonation, 12-15 October 1965, pp. 321-345, Published as ARC-126, by the Office of Naval Research, Department of the Navy, Washington, DC.
7. Dobratz, B. M., "LLNL Explosives Handbook, Properties of Chemical Explosives and Explosives Simulants," Report UCRL-52997, 16 March 1981. Lawrence Livermore National Laboratory, University of California, Livermore, CA 94550.
8. Liddiard, Jr., T. P., and Jacobs, S. J., "Initiation of Reaction in Explosives by Shocks," NOLTR-64-53. 4 October 1965, U.S. Naval Ordnance Laboratory, White Oak, MD.
9. Price, Donna, Clairmont, Jr., A. R., and Erkman, J. O., "The NOL Large Scale Gap Test. III Compilation of Unclassified Data and Supplementary Information for Interpretation of Results." NOLTR-74-40 and AD-780 429, 8 March 1974, U.S. Naval Ordnance Laboratory, White Oak, Silver Spring, MD 20910.

REFERENCES (Continued)

10. Tasker, D. G., "Shock Initiation and Subsequent Growth of Reaction in Explosives and Propellants: The Low Amplitude Shock Initiation Test, LASI." Paper in the Seventh Symposium (International) on Detonation, 16-19 June 1981, pp. 285-298, proceedings published as NSWC MP-82-334 by the Naval Surface Weapons Center, White Oak, Silver Spring, MD 20910.
11. Taylor, B. C., and Ervin, L. W., "Separation of Ignition and Buildup to Detonation in Pressed TNT." Paper presented in the Sixth Symposium (International) on Detonation, 24-27 August 1976, proceedings published as ONR-ACR-221, pp. 3-10, Office of Naval Research, Department of the Navy, Arlington, VA.
12. Howe, P., Frey, R., Taylor, B. C., and Boyle, V., "Shock Initiation and the Critical Energy Concept," paper presented at the Sixth Symposium (International) on Detonation, 24-27 August 1976, proceedings published as ONR-ACR-221, pp. 11-14, Office of Naval Research, Department of the Navy, Arlington, VA.
13. Kroh, M., Thoma, K., Arnold, W., and Wollenweber, U., "Shock Sensitivity and Performance of Several High Explosives," paper presented at the Eighth Symposium (International) on Detonation, 15-19 July 1985, published as NSWC-MP-86-194, pp. 1131-1138, Naval Surface Weapons Center, White Oak, Silver Spring, MD 20903-5000.
14. Bloomquist, D. D., and Sheffield, S. A., "Thermocouple Temperature Measurements in Shock Initiated PBX-9404," paper presented at the Seventh Symposium (International) on Detonation, 16-19 June 1981, pp. 1004-1009, published as NSWC-MP-82-334, Naval Surface Weapons Center, White Oak, Silver Spring, MD 20903-5000.
15. Bloomquist, D. D., and Sheffield, S. W., "Thermocouple Temperature Measurements in Shock-Compressed Solids," Journal of Applied Physics, Vol. 51, No. 10, October 1980, pp. 5260-5266.
16. Crocner, Jean, Jacqueson, Jean, and Migault, Andre, "Anomalous Thermoelectric Effect in the Shock Regime and Application to a Shock Pressure Transducer," paper presented at the Fourth Symposium (International) on Detonation, 12-15 October 1965, published as ACR-126, pp. 627-638, by the Office of Naval Research, Department of the Navy, Washington, DC.
17. Billingsley, J. P., and Yuan, S. W., "An Experimental Investigation of High Velocity Impact," paper published in Applied Scientific Research, Vol. 24, October 1971, pp. 431-451.
18. Walker, F. E., and Wasley, R. J., "Critical Energy for Shock Initiation of Heterogeneous Explosives," Explosivestoffe, No. 1, 1969, p. 9-13.
19. Ayres, J. N., Montesi, L. J., and Bauer, R. J., "Small Scale Gap Test (SSGT) Data Compilation: 1959-1972 Vol. I, Unclassified Explosives," NOLTR-73-132, Vol. I, 26 October 1973. Naval Ordnance Laboratory, White Oak, Silver Spring, MD 20910.

REFERENCES (Concluded)

20. Lindstrom, I. E., "Planar Shock Initiation of Porous Tetryl," Journal of Applied Physics, Vol. 41, No. 1, January 1970, pp. 37-350.
21. Asay, J. R., and Kerley, G. I., "The Response of Materials to Dynamic Loading," Paper in Proceedings of the 1986 Symposium on Hypervelocity Impact, 21-24 October 1986, published as Vol. 5, Nos. 1-4, 1987, of the International Journal of Impact Engineering, pp. 69-99.
22. Duvall, G. E., and Graham, R. A., "Phase Transitions Under Shock Wave Loading," Reviews of Modern Physics, Vol. 49, No. 3, July 1977, pp. 523-579.
23. Boslough, M. B., "Shock Induced Solid-State Chemical Reactivity Studies Using Time Resolved Radiation Pyrometry," paper in the proceedings of the 1986 Symposium on Hypervelocity Impact, 21-24 October 1986, published as Vol. 5, Nos. 1-4 of the International Journal of Impact Engineering, pp. 173-180.

APPENDIX

COMPUTATION OF m_{av} AND $d_{l,av}$ FOR CHEMICAL COMPOUNDS
AND MIXTURES OF COMPOUNDS

The solid materials considered in this study were either chemical compounds (TNT, Tetryl, and PMMA) or mixtures of chemical compounds and pure elements. For these compounds and/or mixtures, the weighted average mass, m_{av} , of a single atom in the material was desired.

First, it was necessary to compute the mass of a single atom for each of the elements contained in the solid. Each solid was composed of one or more, but not all, of the following elements:

Carbon, C; Hydrogen, H; Nitrogen, N;

Oxygen, O; Aluminum, Al; Calcium, Ca;

Chlorine, Cl; Phosphorous, P; Flourine, F.

The mass of a single atom of these elements is:

$$m = \frac{MW}{N_{av}} = \frac{\text{Grams/Gram-Mole}}{\text{Atoms/Gram-Mole}}$$

$$= \frac{\text{Grams}}{\text{Atom}} \quad (A-1)$$

Where:

MW = Molecular Weight, $\frac{\text{Grams}}{\text{Gram-Mole}}$

N_{av} = Avogadros Number

$= 6.02217 \times 10^{23} \frac{\text{Atoms}}{\text{Gram-Mole}}$

Table A-1 lists MW and m for each of the elements in the above list.

To compute the average weight (m_{av}) of an atom in the material, the chemical formula or proportional chemical composition must be known. Of course, the weight (m) of each elemental atom must also be known, since m_{av} is just a weighted average of the elemental atoms in the material.

When m_{av} is computed, then the average space between atoms (d_{1av}) is given by Eq. (9) in the main text.

$$d_{1av} = \left(\frac{m_{av}}{\rho_0} \right)^{1/3} \text{ cm} \quad (9)$$

Computations of m_{av} and d_{1av} for the materials considered in this analysis are shown in the following text. Chemical composition information for the explosives was obtained from [7]. Similar information for the inert material (PMMA) was found in [6]. Values of N_{av} and MW are from various chemistry textbooks and handbooks.

TABLE A-1. Mass Of A Single Atom For Selected Elements.

Element	MW	N_{av}	m
-	<u>Grams</u> <u>Gram-Mole</u>	<u>Atoms</u> <u>Gram-Mole</u>	<u>Grams</u> <u>Atom</u>
Carbon, C	12.011	6.02252(10 ²³)	1.9943(10 ⁻²³)
Hydrogen, H	1.008		0.1674(10 ⁻²³)
Nitrogen, N	14.008		2.3259(10 ⁻²³)
Oxygen, O	16.00		2.6567(10 ⁻²³)
Aluminum, Al	26.98		4.4800(10 ⁻²³)
Calcium, Ca	40.08		6.6554(10 ⁻²³)
Chlorine, Cl	35.45		5.8874(10 ⁻²³)
Phosphorous, P	30.97		5.1432(10 ⁻²³)
Flourine, F	18.9984		3.1546(10 ⁻²³)

Comp - B3: $\rho_o = 1.70 \text{ Grams/cm}^3$

Chemical Composition: C_{2.05} H_{2.51} N_{2.15} O_{2.67}

$$\text{C}_{2.05}, 2.05 * 1.9943 (10^{-23}) = 4.0884 (10^{-23}) \text{ Grams}$$

$$\text{H}_{2.51}, 2.51 * 0.1674 (10^{-23}) = 0.4201 (10^{-23}) \text{ Grams}$$

$$\text{N}_{2.15}, 2.15 * 2.3259 (10^{-23}) = 5.0008 (10^{-23}) \text{ Grams}$$

$$\text{O}_{2.67}, 2.67 * 2.6567 (10^{-23}) = 7.0943 (10^{-23}) \text{ Grams}$$

$$\begin{array}{rcl} \hline 9.38 & \text{Atoms} & \hline 16.6027 (10^{-23}) & \text{Grams} & \hline \end{array}$$

$$m_{av} = \frac{16.6027(10^{-23})}{9.38}$$

$$= 1.7700 (10^{-23}) \frac{\text{Grams}}{\text{Atom}}$$

$$d_{1av}^3 = \frac{m_{av}}{\rho_o} = \frac{1.7700 (10^{-23})}{1.70}$$

$$= 10.4118 (10^{-24}) \text{ cm}^3$$

$$d_{1av} = 2.1839 (10^{-8}) \text{ cm}$$

Comp - B: $\rho_o = 1.70 \text{ Grams/cm}^3$

Chemical Composition: C_{2.03} H_{2.64} N_{2.18} O_{2.67}

$$\text{C}_{2.03}, 2.03 * 1.9943 (10^{-23}) = 4.0484 (10^{-23}) \text{ Grams}$$

$$\text{H}_{2.64}, 2.64 * 0.1674 (10^{-23}) = 0.4419 (10^{-23}) \text{ Grams}$$

$$\text{N}_{2.18}, 2.18 * 2.3259 (10^{-23}) = 5.0705 (10^{-23}) \text{ Grams}$$

$$\text{O}_{2.67}, 2.67 * 2.6567 (10^{-23}) = 7.0934 (10^{-23}) \text{ Grams}$$

$$\begin{array}{rcl} \hline 9.52 & \text{Atoms} & \hline 16.6542 (10^{-23}) & \text{Grams} & \hline \end{array}$$

$$m_{av} = \frac{16.6542 (10^{-23})}{9.52}$$

$$= 1.7494 (10^{-23}) \frac{\text{Grams}}{\text{Atoms}}$$

$$d_{1av}^3 = \frac{m_{av}}{\rho_o} = \frac{17.494 (10^{-24})}{1.70}$$

$$= 10.2906 (10^{-24}) \text{ cm}^3$$

$$d_{1av} = 2.1751 (10^{-8}) \text{ cm}$$

$$\text{TNT: } \rho_o = 1.635 \text{ Grams/cm}^3$$

Chemical Composition: C₇ H₅ N₃ O₆

$$C_7, 7 * 1.9943 (10^{-23}) = 13.9601 (10^{-23}) \text{ Grams}$$

$$H_5, 5 * 0.1674 (10^{-23}) = 0.8370 (10^{-23}) \text{ Grams}$$

$$N_3, 3 * 2.3259 (10^{-23}) = 6.9777 (10^{-23}) \text{ Grams}$$

$$O_6, 6 * 2.6567 (10^{-23}) = 15.9402 (10^{-23}) \text{ Grams}$$

$$\begin{array}{rcl} \hline 21 & \text{Atoms} & \hline & & 37.7150 (10^{-23}) \text{ Grams} \end{array}$$

$$m_{av} = \frac{37.7150 (10^{-23})}{21.0}$$

$$= 1.79595 (10^{-23}) \frac{\text{Grams}}{\text{Atom}}$$

$$d_{1av}^3 = \frac{m_{AV}}{\rho_o} = \frac{17.9595 (10^{-24})}{1.635}$$

$$= 10.9844 \text{ cm}^3$$

$$d_{1av} = 2.2229 (10^{-8}) \text{ cm}$$

PBX - 9404: $\rho_0 = 1.835 \text{ Grams/cm}^3$

Chemical Composition: C_{1.40} H_{2.75} N_{2.57} O_{2.69} Cl_{0.03} P_{0.01}

C _{1.40}	1.40	*	1.9943 (10 ⁻²³)	=	2.79202 (10 ⁻²³)	Grams
H _{2.75}	2.75	*	0.1674 (10 ⁻²³)	=	0.46035 (10 ⁻²³)	Grams
N _{2.57}	2.57	*	2.3259 (10 ⁻²³)	=	5.97756 (10 ⁻²³)	Grams
O _{2.69}	2.69	*	2.6567 (10 ⁻²³)	=	7.14652 (10 ⁻²³)	Grams
Cl _{0.03}	0.03	*	5.8874 (10 ⁻²³)	=	0.17662 (10 ⁻²³)	Grams
P _{0.01}	0.01	*	5.1432 (10 ⁻²³)	=	0.05143 (10 ⁻²³)	Grams
	9.45		Atoms		16.60450 (10 ⁻²³)	Grams

$$m_{av} = \frac{16.6045 (10^{-23})}{9.45}$$

$$= 1.7571 (10^{-23}) \frac{\text{Grams}}{\text{Atom}}$$

$$d_{1av} = \frac{3}{\rho_0} = \frac{m_{av} \cdot 17.571 (10^{-24})}{1.835}$$

$$= 9.5754 (10^{-24}) \text{ cm}^3$$

$$d_{1av} = 2.1235 (10^{-8}) \text{ cm}$$

H-6: $\rho_0 = 1.75 \text{ Grams/cm}^3$

Chemical Composition: C_{1.89} H_{2.59} N_{1.61} O_{2.01} Al_{0.74} Ca_{0.005} Cl_{0.009}

C _{1.89}	1.89	*	1.9943 (10 ⁻²³)	=	3.7692 (10 ⁻²³)	Grams
H _{2.59}	2.59	*	0.1674 (10 ⁻²³)	=	0.4336 (10 ⁻²³)	Grams
N _{1.61}	1.61	*	2.3259 (10 ⁻²³)	=	3.7447 (10 ⁻²³)	Grams
O _{2.01}	2.01	*	2.6567 (10 ⁻²³)	=	5.3400 (10 ⁻²³)	Grams
Al _{0.74}	0.74	*	4.4800 (10 ⁻²³)	=	3.3152 (10 ⁻²³)	Grams
Ca _{0.005}	0.005	*	6.6554 (10 ⁻²³)	=	0.0328 (10 ⁻²³)	Grams

$$\begin{array}{rcl} \text{Cl}_{0.009} & 0.009 * & 5.8874 (10^{-23}) = 0.0530 (10^{-23}) \text{ Grams} \\ & \underline{8.854} & \text{Atoms} \quad \underline{16.6885 (10^{-23})} \text{ Grams} \end{array}$$

$$\begin{aligned} m_{av} &= \frac{16.6885 (10^{-23})}{8.854} \\ &= 1.8849 (10^{-23}) \frac{\text{Grams}}{\text{Atom}} \end{aligned}$$

$$\begin{aligned} d_{1av}^3 &= \frac{m_{av}}{\rho_o} = \frac{18.849 (10^{-24})}{1.75} \\ &= 10.7712 (10^{-24}) \text{ cm}^3 \end{aligned}$$

$$d_{1av} = 2.2085 (10^{-8}) \text{ cm}$$

TETRYL: $\rho_o = 1.68 \text{ Grams/cm}^3$

Chemical Composition: C₇ H₅ N₅ O₈

$$\begin{array}{rcl} \text{C}_7, 7 * & 1.9943 (10^{-23}) = & 13.9601 (10^{-23}) \text{ Grams} \\ \text{H}_5, 5 * & 0.1674 (10^{-23}) = & 0.8370 (10^{-23}) \text{ Grams} \\ \text{N}_5, 5 * & 2.3259 (10^{-23}) = & 11.6295 (10^{-23}) \text{ Grams} \\ \text{O}_8, 8 * & 2.6567 (10^{-23}) = & 21.2536 (10^{-23}) \text{ Grams} \\ \underline{25} & \text{Atoms} & \underline{47.6802 (10^{-23})} \text{ Grams} \end{array}$$

$$\begin{aligned} m_{av} &= \frac{47.6802 (10^{-23})}{25} \\ &= 1.9072 (10^{-23}) \frac{\text{Grams}}{\text{Atom}} \end{aligned}$$

$$\begin{aligned} d_{1av}^3 &= \frac{m_{av}}{\rho_o} = \frac{19.072 (10^{-24})}{1.68} \\ &= 11.3524 (10^{-24}) \text{ cm}^3 \end{aligned}$$

$$d_{1av} = 2.2475 (10^{-8}) \text{ cm}$$

POLYMETHYL - METHACRYLATE (PMMA)
(PLEXIGLAS TYPE II, UVA)

$$\rho_o = 1.18 \frac{\text{Gram}}{\text{cm}^3}$$

Chemical Composition: $(C_5 H_8 O_2)_N$

$$C_5, 5 * 1.9943 (10^{-23}) = 9.9715 (10^{-23}) \text{ Grams}$$

$$H_8, 8 * 0.1674 (10^{-23}) = 1.3392 (10^{-23}) \text{ Grams}$$

$$O_2, 2 * 2.6567 (10^{-23}) = 5.3134 (10^{-23}) \text{ Grams}$$

$$\begin{array}{rcl} \overline{15} & \text{Atoms} & \overline{16.6241 (10^{-23})} \text{ Grams} \end{array}$$

$$m_{av} = \frac{16.6241 (10^{-23})}{15.0}$$

$$= 1.1083 (10^{-23}) \frac{\text{Grams}}{\text{Atom}}$$

$$d_{1av}^3 = \frac{m_{av}}{\rho_o} = \frac{11.083 (10^{-24})}{1.18}$$

$$= 9.3924 (10^{-24}) \text{ cm}^3$$

$$d_{1av} = 2.1099 (10^{-8}) \text{ cm}$$

DISTRIBUTION

	<u>No. of Copies</u>
Sandia National Laboratories ATTN: Dr. D. D. Bloomquist P. O. Box 5800 Division 1252 Albuquerque, NM 87185	3
Los Alamos National Laboratory ATTN: Dr. Steven A. Sheffield Group M-9 Mail Stop T-959 Los Alamos, NM 87545	3
Antiarmor Munitions Technical Office ATTN: AMCLO-AM, Dr. P. Howe Building 328 Aberdeen Proving Ground, MD 21005-5066	3
Explosives Effects Branch ATTN: SLCBR-TB-EE, Dr. R. Frey Aberdeen Proving Ground, MD 21005-5066	3
Los Alamos National Laboratory ATTN: Dr. I. E. Lindstrom Group WX-5 Mail Stop G-780 Box 1663 Los Alamos, NM 87545	3
Naval Surface Weapons Center ATTN: R12, Mr. J. M. Short White Oak Silver Spring, MD 20903-5000	3
Naval Surface Warfare Center ATTN: Mr. Tom Wasmund Code G-13 Dahlgren, VA 22448	3
Eglin Air Force Base ATTN: AD/CZL, Mr. Bill Dyess Eglin AFB, FL	1
Eglin Air Force Base ATTN: AD/ALJW, Dr. Joe Foster Eglin AFB, FL	2
U.S. Army Materiel Systems Analysis Activity ATTN: AMXSY-MP Aberdeen Proving Ground, MD 21005	1

DISTRIBUTION (Cont'd)

	<u>No. of Copies</u>
IIT Research Institute ATTN: GACIAC Mr. A. J. Tulis 10 W. 35th Street Chicago, IL 60616	2
TASC ATTN: Mr. Charles E. Clucus 907 Mar-Walt Drive Fort Walton Beach, FL 32548	2
University of Alabama at Huntsville (UAH) Research Institute ATTN: Mr. C. L. Adams Dr. B. Z. Jenkins Huntsville, AL 35816	5 1
Johns Hopkins University ATTN: Professor E. R. Fitzgerald 127 Latrobe Hall 34th and Charles Street Baltimore, MD 21218	3
McGill University Department of Mechanical Engineering ATTN: Professor J. H. Lee 817 Sherbrooke West Montreal, Canada H3A 2K 6	3
University of Illinois Department of Aeronautical and Astronautical Engineering ATTN: Professor R. A. Strehlow Urbana, IL 61801	3
Franco - German Institute Saint Louis (ISL) ATTN: Mr. Henry P. A. Moulard 12 Rue De L'Industrie Saint Louis, France 68300	3
One Daniel Burnham Court ATTN: Dr. S. W. Yuan Apartment 1222 San Francisco, CA 94109	2

DISTRIBUTION (Concluded)

	<u>No. of Copies</u>
AMCPM-PA-JTMD, BG Capps	1
AMCPM-PA-SE, COL Flick	1
Mr. Don Adams	1
AMCPM-HA, COL Liberatore	1
AMCPM-HA-SE, Mr. James Harchanko	1
AMCPEO-CM, Mr. Jerry Brown	1
AMSMI-RD, Dr. McCorkle	1
Dr. Rhoades	1
Dr. Stephens	1
AMSMI-RD-RE, Dr. R. L. Hartman	1
AMSMI-RD-SS, Dr. Grider	1
Mr. Davis	1
AMSMI-RD-SS-SE, Mr. Grabney	1
Mr. Jordan	1
Mr. Grabney	1
Mr. Waddle	1
AMSMI-RD-SS-SS, Dr. Billingsley	10
Mr. Head	1
Dr. Oliver	1
Mr. Harris	1
AMSMI-RD-ST-WF, Mr. Schexnayder	1
Mr. Lovelace	1
Mr. Lienau	1
Ms. Brantley	1
Mr. Hill	1
Mr. Cornelius	1
Mr. MacDonald	1
AMSMI-RD-CS-R	15
AMSMI-RD-CS-T	1
AMSMI-GC-IP, Mr. Fred Bush	1